Deconvoluting chain heterogeneities from driven translocation through a nano-pore

Ramesh Adhikari and Aniket Bhattacharya*
Department of Physics, University of Central Florida, Orlando, Florida 32816-2385, USA
(Dated: February 3, 2015)

We study translocation dynamics of a driven compressible semi-flexible chain consisting of alternate blocks of stiff (S) and flexible (F) segments of size m and n respectively for different chain length N in two dimension (2D). The free parameters in the model are the bending rigidity κ_b which controls the three body interaction term, the elastic constant k_F in the FENE (bond) potential between successive monomers, as well as the segmental lengths m and n and the repeat unit p ($N = m_p n_p$) and the solvent viscosity γ. We demonstrate that due to the change in entropic barrier and the inhomogeneous viscous drag on the chain backbone a variety of scenarios are possible amply manifested in the waiting time distribution of the translocating chain. These information can be deconvoluted to extract the mechanical properties of the chain at various length scales and thus can be used to nanopore based methods to probe bio-molecules, such as DNA, RNA and proteins.

PACS numbers: 87.15.ap, 82.35.Lr, 82.35.Pq

arXiv:1405.7013v4 [physics.bio-ph] 2 Feb 2015

Polymer translocation (PT) through a nano-pore (NP) is being explored for more than a decade as a NP based device has the potential to provide single molecule detection when a DNA is driven electrophoretically through a NP [1, 2]. Unlike traditional Sanger's method [3] this does not require amplification; thus one can in principle analyze a single genome [4]. Progress towards this target offers challenges to overcome which have attracted a lot of attention from various disciplines of sciences and engineering [5, 6]. A large fraction of theoretical and numerical studies have been devoted to translocation studies of flexible homo-polymers [1, 2]. However, to extract sequence specific information for a DNA or a protein, as they translocate and/or unfold through a nanopore, one needs generalization of the model to account for how different segments of the translocating polymer interact with the pore or the solvent. Translocation of the heterogeneous polymer has been studied in the past for a fully flexible polymer where different segments encounter different forces [7–10]. For periodic blocks one observes novel periodic fringes from which information about the block length can in principle be readily extracted [7, 8]. Recently, de Haan and Slater [11] have studied translocation of rod-coil polymer through a nanopore in the *quasi-static limit* (weakly driven through narrow pore and negligible fluid viscosity). They have used incremental mean first passage time (IMFPT) [12] approach and verified that in the quasi-static limit the stiff and flexible segments can be discriminated due to local entropic mismatch between the stiff and flexible segments reflected in the steps and plateaus of the IMFPT of different segments.

In this letter we provide new insights for the driven heterogeneous PT through a NP where heterogeneity is introduced by varying both the *bond bending* as well as the *bond stretching* potentials. We study the translocation dynamics in the presence of large fluid viscosity and strong driving force so that the system is not in the quasi-static limit as in Ref. [11]. Our studies are motivated by the observation that many bio-polymers, such as DNA and proteins exhibit helical and random coil segments whose elastic and bending properties are very different, so is the entropic contribution due to very different number and nature of polymeric conformations. It is also likely that a double stranded (ds) DNA can be in a partially melted state whose coarse-grained description will require nonuniform bond bending and bond-stretching potentials for different regions. As a result, if one wants to develop a NP based device to detect and identify the translocating segments, a prior knowledge of their residence inside the pore will be extremely useful. Naturally, the length scale of the heterogeneity $\xi(n, m)$, where m and n are the lengths of the stiff and flexible segments respectively in each block, will obviously be an important parameter for the analysis of the translocation problem. Thus, we first show that a proper coarse graining of the model in units of ξ will lead to the known results for the homopolymer translocation. Then we further analyze the results at the length scale of the blob size ξ and show how the chain elasticity and the chain stiffness introduce fine prints in the translocation process. We explain our findings using Sakaue's non-equilibrium tension propagation (TP) theory [13] recently verified for a CG models of semi-flexible chain by us [14–16]. We have used Lennard-Jones (LJ), Finitely Extensible Nonlinear Elastic (FENE) spring potential and a three body bond bending potential to mimic excluded volume (EV), bond stretching between two successive monomers, and stiffness of the chain respectively, and applied a constant external force ($F_{ext} = 5.0$) at the pore in the translocation direction. We have used the Brownian dynamics (BD) scheme to study the heterogeneous PT problem. The details of the BD methods are the same as in our recent publications [14, 15]. Initially we keep the elastic spring constant (k_F) to be the same throughout the chain and choose the bending stiffness $\kappa_b = 0$ and 16.0

for the fully flexible and the stiff segments respectively. Later we show that by making the elastic potential for the relatively more flexible part weaker one can reverse the relative friction on the chain segments which results in novel waiting time distributions serving as the fingerprint of the structural motifs translocating through the pore.

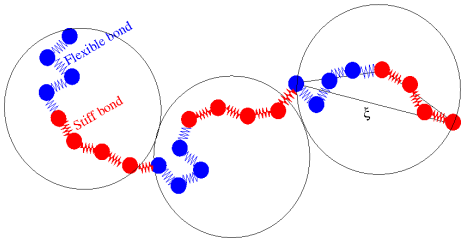

FIG. 1. Blob model of a polymer chain of chain length (N = 24) and segmental length (m = 4). Each repeated unit can be considered as a single blob of length $\xi \sim m^{\beta}$. Please see the text below.

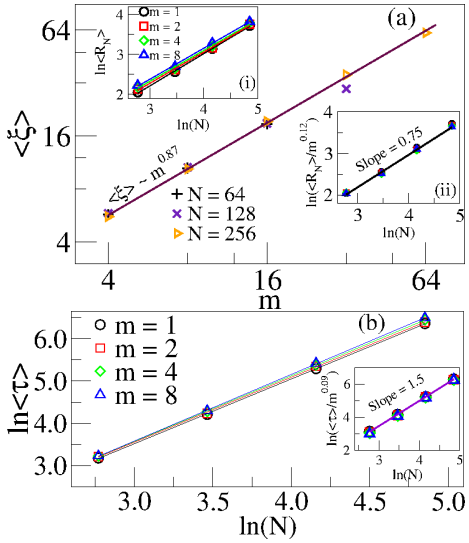

FIG. 2. (a) Log-log plot of blob-size $\langle\xi\rangle$ as a function of m for N = 64 (black plus), N = 128 (violet cross) and N = 256 (orange right-triangle). The solid line represents $\langle\xi\rangle \sim m^{0.87}$. Insets: (i) log-log plot of $\langle R_N\rangle$ as a function of N for different m, (ii) collapse of $\langle R_N\rangle/m^{0.12} \sim N^{\nu}$ on the same master plot. (b) Log-log plot of $\langle\tau\rangle$ as a function of N for different m. Inset: scaling and collapse of $\langle\tau\rangle/m^{0.09} \sim N^{2\nu}$.

• *Blobsize and scaling*: We consider heterogeneous chains consisting of alternate symmetric ($m = n$) periodic blocks of stiff and flexible segments of m monomers so that the block-length is $2m$ (m = 1,2,3,4) as shown in Fig. 1. First we investigate how the alternate stiff and flexible segments of equal length affect the end-to-end distance $\langle R_N(m)\rangle$ and the mean first passage time (MFPT) as a function of the periodic block-length (Fig. 1), compared to a homo-polymer of equal contour length N. To a first approximation one can think of this chain as a flexible chain of $N/2m$ segments, of certain blob size ξ. The blob size ξ in general will be a function of the block-length and bending rigidity of the flexible and stiff segments. For our particular choice of bending rigidity for the flexible ($\kappa_b = 0$) and stiff ($\kappa_b = 16$) segments from simulation results for $N = 64 - 256$ we find an expected power law scaling $\xi \sim m^{\beta}$ where $\beta = 0.87$ (Fig. 2). Obviously the exponent β is non-universal as it depends on κ_b and k_F, but the universal aspects of the entire chain can be regained through scaling with ξ as shown in Fig. 2. The conformation statistics of this basic unit ξ controls both the conformation and translocation properties of the entire chain as follows. We can write $\langle R_N\rangle \equiv \langle\sqrt{R_N^2}\rangle \sim \langle\xi\rangle(N/2m)^{\nu} \sim m^{\beta}N^{\nu}/m^{\nu}$, where ν is the Flory exponent. This implies $\langle R_N\rangle/N^{\nu} \sim m^{\beta-\nu} = m^{0.12}$ (where $\nu = 0.75$ is the Flory exponent in 2D). Simulation data in the insets of Fig. 2(a) confirms our scaling prediction. Likewise, we show that the MFPT $\langle\tau\rangle/N^{2\nu} \sim m^{0.09}$. For small N it has been found earlier that $\langle\tau\rangle \sim \langle R_N\rangle/N^{-\nu} \sim N^{2\nu}$ [17]. Therefore, as expected by proper coarse graining by the elemental block we get back the results for the fully flexible chain. We now show how characteristics of translocation are affected by the chain heterogeneity.

• *Effect of chain heterogeneity on translocation*: In presenting the results we use the notation $(F_mS_n)_p/(S_mF_n)_p$ to denote p blocks of an ordered flexible/stiff and stiff/flexible segments of length m and n respectively ($N = (m+n)p$) and that the flexible/stiff segment enters the pore first. Fig. 3 and Fig. 4 reveal quite a few novel results that we explain using TP theory. For small block-length the order in which the chain enters the pore (either stiff or flexible segment) neither make a big difference in the shape of the histogram (Fig. 3(a)) nor in the MFPT (Fig. 4). For larger block lengths the difference between the histograms for S_mF_m and F_mS_m are quite clear and the dependence of τ on m are also different as seen in Fig. 4. For the case when the stiff portion enters the pore first, the MFPT monotonically increases but in the other case it shows a maximum (Fig. 4). We now explain this in terms of our recent analysis of the translocation of semi-flexible chain using TP theory where we showed that a stiffer chain takes a longer time to translocate [14–16]. When the block lengths are small, TP gets intermittently hindered as the tension propagates through alternate stiff and flexible regions. For longer blocks tension can propagate more effectively unhindered for a longer time. Therefore, when a long stiff segment enters the pore first it increases the MFPT. But, when a long flexible segment enters the pore first it decreases the MFPT. This results a maximum in the $\langle\tau\rangle/\langle\tau\rangle_0$ *vs.* m curve for the FS orientation. The difference of MFPT for S_mF_m and F_mS_m becomes maximum when $m = N/2$. For relatively longer block lengths it makes a big difference in MFPT.

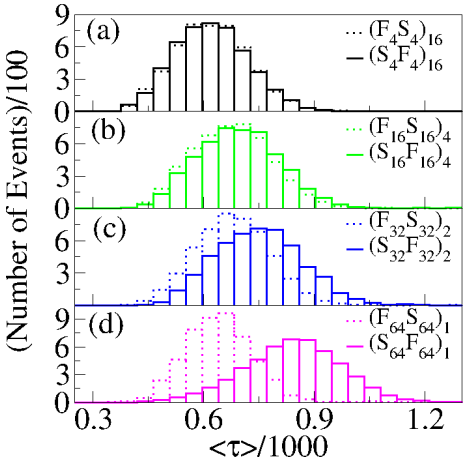

FIG. 3. Histograms of first passage time for chain length $N = 128$ and segmental length (a) $m = 4$, (b) $m = 16$, (c) $m = 32$, and (d) $m = 64$. The dotted/solid lines represent the flexible(F_mS_m)/stiff(S_mF_m) segment entering the pore first. For larger block size the effect of order of entry is clearly visible.

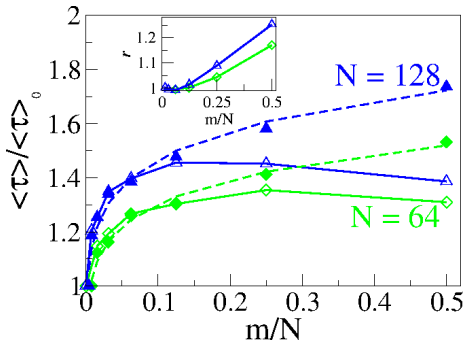

FIG. 4. MFPT (scaled by the MFPT of respective flexible homo-polymer) for chains F_mS_m and S_mF_m as a function of m/N for chains $N = 64$ (green diamonds) and $N = 128$ (blue up-triangles). The open/closed symbols correspond to flexible/stiff segment entering the pore first. The inset shows the ratio of the MFPT for SF to FS orientation. The nanopore is capable of differentiating if a flexible (F) block or a stiff (S) block entered the pore first.

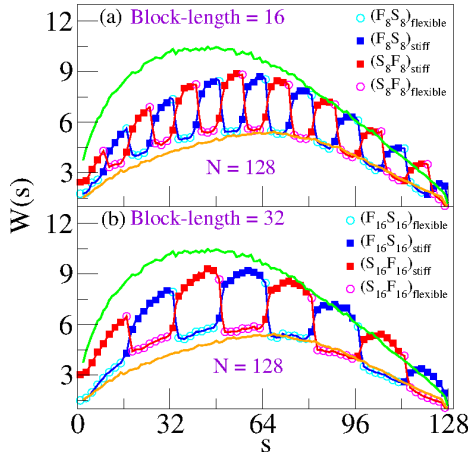

FIG. 5. Waiting time distribution for a $N = 128$ chain with the block-length (a) 16 and (b) 32. Azure (open circles) and Blue (filled squares) correspond to the flexible and stiff segments when the *flexible segment enters the pore first* (F_mS_m). Magenta (open circles) and Red (filled squares) correspond to the flexible and stiff segments when *the stiff segment enters the pore first* (S_mF_m). The solid green and orange lines correspond to the waiting time distributions for the corresponding stiff ($\kappa_b = 16.0$) and fully flexible ($\kappa_b = 0.0$) homo-polymers respectively.

• *Waiting time distribution*: The total time spent by a monomer inside the pore is defined as its waiting time $W(s)$, where s is the index of monomer inside the pore (translocation coordinate). Sum of the waiting time for all monomers is the MFPT *i.e.* $\sum_{s=1}^{N} W(s) = \langle\tau\rangle$. The effect of TP in stiff and flexible parts becomes most visible in the waiting time distribution of the individual monomers of the chain as shown in Fig. 5. We notice that the envelopes for the corresponding homo-polymers for a fully flexible chain ($\kappa_b = 0$, solid orange line) and for the stiffer chain ($\kappa_b = 16$, solid green line) respectively serve as bounds for the heterogeneous chains [22]. As explained in our previous publication [15] the TP time corresponds to the maximum of these curves and shifts toward a lower s value for a stiffer chain. Bearing this in mind we can reconcile the fringe pattern in the light of the TP theory. The pattern has the following features: (i) The number of fringes is equal to the number of blocks. This is because on an average stiffer portions take longer time to translocate. (ii) The fringes for S_mF_m and F_mS_m are out of phase for the same reason. (iii) The chain heterogeneity affects the waiting distribution most at an early time; beyond the largest TP time (*i.e.*, the peak position of the envelope for $\kappa_b = 0$) the waiting time of the individual monomers (excepting which are at the border separating the stiff and flexible segments) becomes identical to that of the corresponding homogeneous chain. This again exemplifies to analyze the driven translocation as a *pre* and *post* TP events. Please note that the maxima of the $W(s)$ for the heterogeneous chain lie in between the maxima for the corresponding homogeneous cases.

• *Effect of friction and driving force*: In Fig. 5 we chose a value of the solvent friction associated to each monomer $\gamma = 0.7$ for which we find that a stiffer segment translocates slower through the pore. We now discuss how a variation of the solvent friction will affect this conclusion. We first show that the MFPT of a homopolymer of certain length exhibits a crossover as one varies the solvent viscosity (Fig. 6(a)). It is only for extremely small γ (*quasi-static limit*) the stiffer segment translocates faster as studied in [11]. We also have reproduced the result for a particular set of parameters (black line in Fig. 6(b)). We have shown 3D (instead of 2D) data in Fig. 6(b) and (c) only for better resolution. This crossover effect can be explained using Sakaue's tension propagation (TP)

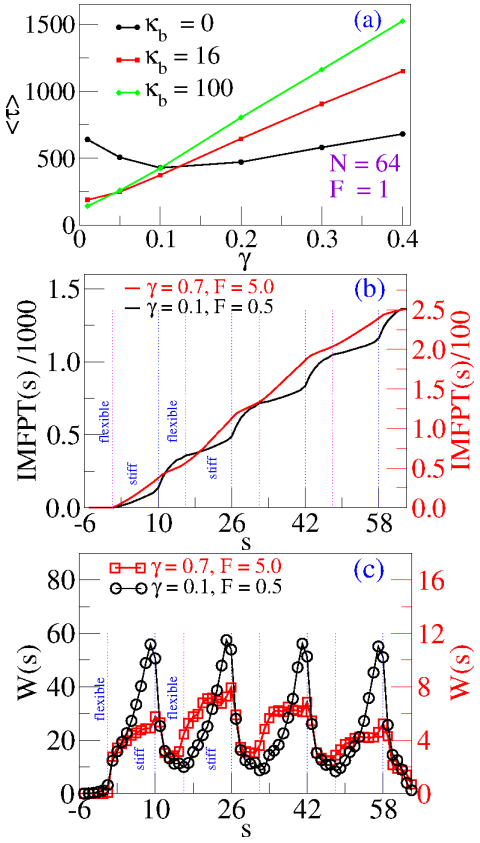

FIG. 6. (a) The MFPT for flexible and semi-flexible homopolymers of length $N = 64$ as a function of solvent-monomer friction γ. (b) The IMFPT and (c) the waiting time distribution as a function of s-coordinate for a chain ($N = 70$) in 3D with four stiff segments ($\kappa_b = 100$) each of length ($m = 10$) and five flexible segments ($\kappa_b = 0$) each of length ($n = 6$) provided that (for (b) and (c)) the first flexible segment is already in the *trans*-side at $t = 0$.

theory [13]. When we use a larger value of γ (implying stiffer segment translocates slower) and/or a bias F the IMFPT changes qualitatively (Fig. 6(b)), which is more prominently seen in the waiting time distribution of the individual monomers (Fig 6(c)).

Using formulae for solvent friction from the bulk $\Gamma_{\rm solv} = \gamma N^{\nu}$ and pore friction $\Gamma_{\rm pore} \sim \frac{A_{pore}}{d-1} + p\gamma$ which have been discussed in Ref. [18, 19] we have checked that $\gamma = 0.7$ and $\gamma = 0.1$ (for the chain lengths used in our simulation) correspond to solvent dominated and pore friction dominated regimes respectively. At high $\Gamma_{\rm solv}$, de-Haan and Slater showed that the MFPT increases linearly with γ [20] for a fully flexible chain. We see the same trend to be valid also for semi-flexible chains, albeit beyond a critical value (Fig. 6(a)). But at low $\Gamma_{\rm solv}$, the dependence of MFPT on γ becomes non-monotonic and it exhibits a minimum for $\gamma = \gamma_m$ [21]. This γ_m marks the onset of change in the qualitative behavior of IMFPT or the waiting time distribution of the individual monomers.

In quasi-static limit, significantly larger local entropic barrier of a "coil" segment causes longer residence time. This effect is reflected as steps in the IMFPT (Fig. 6(b)) and peaks in the waiting time distribution (Fig. 6(c)). But for the non-equilibrium situation, when the stiffer segment enters the pore, tension propagates faster along the chain backbone [13, 15] and more monomers in the *cis*-side set in motion. For large solvent friction this may produce larger viscous drag dominating over local entropic barrier resulting in the stiffer segments translocating slower than the flexible segment. In this case the peaks in the waiting time distribution disappear (red color in Fig. 6(c)). Accordingly, one sees qualitative changes in the corresponding IMFPT (red color in Fig. 6(b)). Therefore, the relative fast/slow translocation of rod /coil segments through the nanopore depends on the relative values of pore friction, solvent friction, and applied bias.

• *Heterogeneous chain with a variable spring constant*: Finally we have extended these studies to see the consequences of allowing the elastic potential between the successive beads to be different in each block. This situation may occur when individual building blocks are connected by linkers of different elasticity. Fig. 7 shows the various combination of the spring constants k_F for the heterogeneous chain. The first four graphs Fig. 7(a)-(d) correspond to the waiting time distribution for the chain with equal number of monomers in each of the flexible and stiff segments. Fig. 7a is the graph where all the F and S segments have the same $k_F = 100$ qualitatively similar to Fig. 5. In Figs. 7(a)-(d) one can see the effect of reduced value of k_F for the flexible portion only.

Figs. 7(e)-(f) represent the waiting time distributions for the unequal length of the flexible and stiff segments. The flexible segment, being shorter, looses the conformational entropic height but the contribution of the FENE force in the direction of translocation is enhanced. We can see the effect of this enhancement in the increased back and forth motion (low frequency phonons of larger amplitude to softer bonds) of the chain towards the translocation direction. The smaller is the value of k_F the larger will be the amplitude of the phonons mode which results in a longer translocation time. Therefore, when we reduce the strength of the FENE interaction for the coil, the coil translocates slower and we got the waiting time distribution picture inverted for the stiff and flexible segments as seen from a comparison of Fig. 7(a) to Fig. 7(d). This will be most prominent if the stiff segments were chosen as rigid rods.

Fig. 7(c)-(f) show the end monomer of each semi-flexible segment has a larger waiting time. This indicates a larger barrier height for the flexible segments. Once the barrier is overcome by the first monomer of the flexible segment, all the following monomers of the flexible segments pass through the pore faster. The end monomer

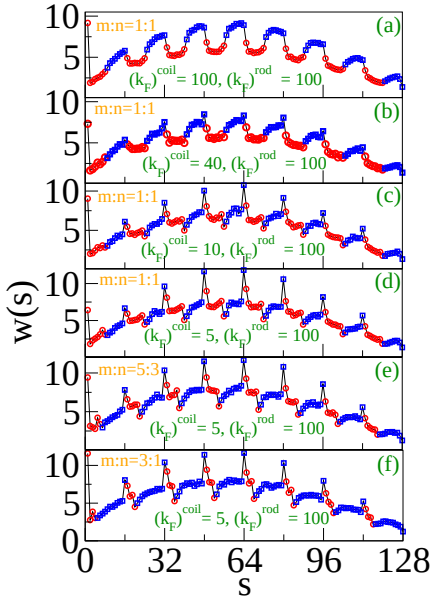

FIG. 7. The waiting time distribution as a function of s-coordinate for a chain ($N = 128$) with variable k_F and stiff-flexible segmental length ratio (m/n). The bending stiffness κ_b for flexible (red circles) and stiff (blue squares) segments are 0 and 16 respectively. The elastic stiffness (k_F) is 100 for stiff segments [(a)-(f)]. For flexible segments (a) $k_F = 100$ (b) $k_F = 40$ (c) $k_F = 10$ (d) $k_F = 5$ (e) $k_F = 5$ and (f) $k_F = 5$. The stiff and flexible segments are of equal length except in (e) $m\colon n = 5\colon 3$ and (f) $m\colon n = 3\colon 1$.

of the flexible segment and the first monomer of the stiff segment have the lowest waiting time which means that they have negligible barrier to overcome. Furthermore a visual comparison of Fig. 5 and Fig. 7 shows that the origin of the details of the waiting time distributions possibly be differentiated by a spectral decomposition analysis of the waiting time distribution.

To summarize, we have demonstrated how a nanopore can sense structural heterogeneity of a bio-polymer driven through a nanopore. Not only do monomers belonging to the flexible and stiff part exhibit different waiting time distributions, we have also demonstrated how a nanopore can sense which end of the polymer enters the pore first. Translating this information for a dsDNA will imply that the nanopore can differentiate the 3-5 or 5-3 ends of a translocating DNA. We have explained these results using the concepts of TP theory. We have clearly demonstrated how the fluid viscosity and an external bias can affect the relative speed of the stiff and flexible segments. Furthermore, unlike previously reported studies [11] we, for the first time, analyzed the interplay of the effects of polymer heterogeneity caused by the variation of elastic and bending stiffness. We have demonstrated that softer elastic bonds raise the MFPT [23]. Therefore, an increase in waiting time for a stiff segment can be compensated by the waiting time for a flexible segment but having softer elastic bonds. This observation can be exploited to tune to control the passage of polymers through NP. It is interesting to note from Fig. 7 that the variation in waiting time distribution arising out of the bending stiffness variation and bond length variation can be differentiated. Therefore, these patterns can serve as references to characterize structural heterogeneity of an unknown polymer translocating through a nanopore. We hope the results reported in this letter will be helpful in deciphering translocating characteristic of bio-polymers observed experimentally.

This research has been partially supported by a UCF College of Science Seed grant. We thank Profs. Gary Slater and Hendrick de Hann for useful discussions.

* Author to whom the correspondence should be addressed; aniket@physics.ucf.edu

[1] M. Muthukumar *Polymer Translocation* (CRC Press, Boca Raton, 2011).
[2] A. Milchev, J. Phys. Condens. Matter **23**, 103101 (2011).
[3] F. Sanger and A. R. Coulson, J. Mol. Biol. **95**, 441 (1975); F. Sanger, S. Nicklen, and A. R. Coulson, Proc. Natl. Acad. Sci. USA **74**, 5463 (1977).
[4] E. R. Mardis, Nature **470**, 198 (2011).
[5] L. Movileanu, Soft Matter **4**, 925 (2008).
[6] D. Rodriguez-Larrea and H. Bayley, Nat. Nanotech. **8**, 288 (2013).
[7] K. Luo, T. Ala-Nissila, S.C. Ying and A. Bhattacharya, J. Chem. Phys. **126**, 145101 (2007).
[8] K. Luo, T. Ala-Nissila, S.C. Ying and A. Bhattacharya, Phys. Rev. Lett. **100**, 058101 (2008).
[9] M. G. Gauthier and G. W. Slater, J. Chem. Phys. **128**, 175103 (2008).
[10] S. Mirigan, Y. Wang, and M. Muthukumar, J. Chem. Phys. **137**, 064904 (2012).
[11] H. W. de Hann and G. W. Slater, Phys. Rev. Lett. **110**, 048101 (2013).
[12] H. W. de Hann, G. W. Slater, J. Chem. Phys. **134**, 154905 (2011).
[13] T. Sakaue, Phys. Rev. E **76**, 021803 (2007); *ibid* **81**, 041808 (2010).
[14] A. Bhattacharya, J. Polymer Science Series C **55**, 60-69 (2013).
[15] R. Adhikari and A. Bhattacharya, J. Chem. Phys. **138**, 204909 (2013).
[16] Sakaue's TP picture was demonstrated to be valid for a fully flexible chain by translating the original theory to a BD scheme [18, 24]. In refs. [14, 15] we discussed how the TP picture will be affected by the stiffness of the chain.
[17] K. Luo, I. Huopaniemi, T. Ala-Nissila, and S.-C. Ying, J. Chem. Phys. **124**, 114704 (2006).
[18] T. Ikonen, A. Bhattacharya, T. Ala-Nissila and W. Sung, J. Chem. Phys. **137**, 085101 (2012).
[19] T. Ikonen, A. Bhattacharya, T. Ala-Nissila, and W. Sung, Europhys. Lett. **103**, 38001 (2013).
[20] H. W. de Haan and G. W. Slater, J. Chem. Phys. **136**, 154903 (2012)

[21] R. Adhikari and A. Bhattacharya, Unpublished.
In the pore friction dominated regime upon decreasing the solvent viscosity the system is closer to its equilibrium state and the translocation dynamics is determined by entropic barrier crossing. This entropic barrier is smaller for a stiffer chain and becomes negligible for rod-like polymer. At low viscosity, the force due to pore friction increases as the solvent viscosity decreases resulting in an increase in the MFPT which explains the minimum of the MFPT at a particular viscosity $\gamma \sim \gamma_m$.

[22] This characteristic pattern of waiting time distribution seems to be a generic feature as it was seen earlier for segments under different bias [7] or due to different pore-segment interaction [8].

[23] We have simulated driven translocation of a one dimensional compressible chain and find that the MFPT with the elastic constant k_F increases as $\langle \tau \rangle \sim N^2 k_F^{-1/8}$.

[24] T. Ikonen, A. Bhattacharya, T. Ala-Nissila and W. Sung, Phys. Rev. E **85**, 051803 (2012).